PROCEEDINGS OF SCIENCE

A new experiment on the ^{2}H(α,γ)^{6}Li reaction

Michael Anders[*†]
Helmholtz-Zentrum Dresden-Rossendorf
E-mail: m.anders@hzdr.de

The ^{2}H(α,γ)^{6}Li cross section has been measured by in-beam γ-spectrometry at the deep underground 400 keV LUNA accelerator in Italy's Gran Sasso laboratory. An alpha-beam of 280-400 keV energy was incident on a windowless deuterium gas target, and the γ rays from the reaction were detected in a large high-purity germanium detector. Due to elastically scattered deuterons, there is a low but not negligible parasitic neutron production of the order of 10 neutrons per second. These neutrons give rise to a significant background in the germanium detector. In addition to the underground in-beam experiment, studies using americium-beryllium and deuterium-deuterium neutron sources and Monte Carlo simulations have been performed. The analysis of signal and background is described in detail.

XII International Symposium on Nuclei in the Cosmos,
August 5-12, 2012
Cairns, Australia

[*]Speaker.
[†]for the LUNA collaboration

PoS(NIC XII)137

1. Introduction

For 30 years now, the cosmological lithium puzzle has frustrated the efforts of observers and cosmologists [1, a recent review]. Observations in metal-poor stars consistently show a factor of two or three lower abundance of the main stable lithium isotope ^{7}Li than what is predicted by standard Big Bang nucleosynthesis, even though some possible stellar solutions have been suggested [2]. Recent observations of the second stable lithium isotope ^{6}Li in metal-poor stars have introduced a possible additional puzzle concerning cosmological ^{6}Li. The observed ^{6}Li/^{7}Li abundance ratio of about 0.05 [3] largely exceeds the standard Big Bang nucleosynthesis prediction. Even though many of the claimed ^{6}Li detections may be in error [4, 5], for a few metal-poor stars [6] there still seems to be a ^{6}Li isotopic abundance of a few percent [7]. These observations are much higher than the predicted ^{6}Li yield from standard Big Bang nucleosynthesis [8]. ^{6}Li is much more easily depleted through nuclear reactions than its more abundant sister isotope ^{7}Li [9], and non-cosmological scenarios for significant ^{6}Li production all co-produce ^{7}Li and thus worsen the ^{7}Li problem [10, a very recent example]. Therefore, the detections of ^{6}Li in very old stars raise the question of a possible cosmological production. However, with standard Big Bang nucleosynthesis producing much too little ^{6}Li [8], all cosmological scenarios producing enough ^{6}Li involve non-standard physics [11, 12, 13, 14]. Before studying such exotic scenarios, it is important to first determine precisely how much ^{6}Li can be produced in standard Big Bang nucleosynthesis. With this experimental baseline, any missing additional ^{6}Li provided by non-standard approaches can be quantified.

The ^{2}H(α,γ)^{6}Li reaction is the dominant nuclear reaction for ^{6}Li production in standard Big Bang nucleosynthesis [8]. At the energies relevant for Big Bang nucleosynthesis, E $\approx$ 50-300 keV, the ^{2}H(α,γ)^{6}Li cross section is very small. Therefore, it has never been measured experimentally at such low energies, and theoretical predictions remain uncertain [15]. The reaction has been studied previously by in-beam-spectrometry around and above the E = 0.711 MeV resonance [16, 17, 18]. Two attempts to determine the ^{2}H(α,γ)^{6}Li cross section also below the resonance have been made using the Coulomb dissociation technique [19, 20]. This method is especially sensitive to quadrupole (E2) transitions in the excited ^{6}Li nucleus, largely neglecting dipole transitions. It is furthermore limited by possible background from non-Coulomb, i.e. nuclear breakup [21], so these data should be interpreted as upper limits [20]. Therefore, direct data on the ^{2}H(α,γ)^{6}Li cross section at Big Bang energies are still needed. A new experiment at the Laboratory for Underground Nuclear Astrophysics (LUNA) may provide the required data.

The experiment was performed at the LUNA 400 kV accelerator in the Gran Sasso laboratory, Italy (LNGS). This facility is shielded from cosmic-rays by the Gran Sasso mountain, reducing the muon flux by six orders of magnitude [32]. The ambient flux of energetic neutrons at Gran Sasso is of the order of 10^{-6} s^{-1} cm^{-2} [33, 34], three orders of magnitude lower than at the surface of the Earth. LUNA is the world's only underground accelerator facility. It is dedicated to measuring the cross section of astrophysically relevant reactions well below the Coulomb barrier [35, 36], taking advantage of its ultra-low background [37, 38, 39].

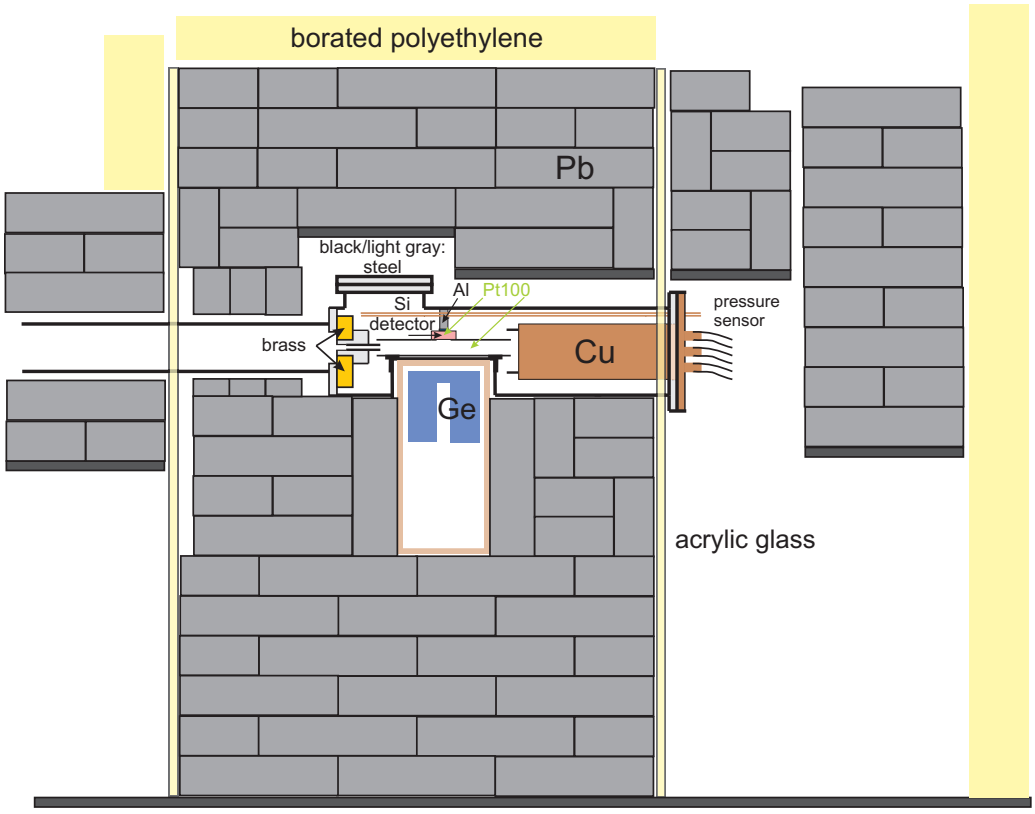

Figure 1: Experimental setup, as seen from the side. The central chamber of the windowless gas target is seen near the center of the plot. The α-beam enters the target from the left through a 4 cm long collimator of 7 mm inner diameter and is stopped on a massive copper beam calorimeter. The germanium (for γ rays) and silicon (for charged particles) detectors are also shown, as well as the Pt100 temperature sensors and the tube leading to the capacitive pressure sensor. The setup is surrounded by a lead castle and walls of borated polyethylene. The inner lead castle is surrounded by an anti-radon box made of acrylic glass.

2. The LUNA setup - a windowless 0.3 mbar deuterium gas target

On the LUNA beam line for gaseous targets, a collimated $^4He^+$ beam (280 and 400 keV, up to 360 μA) was incident on a windowless $^2H_2$ target with a typical working pressure of 0.3 mbar. The beam current was measured by a calorimeter made of copper, the gas pressure by a precise capacitive pressure sensor. The target chamber was made of steel and had a recess to site the HPGe detector very close to the beam. This ultra-low background high-purity germanium detector with a high relative efficiency of 137 % measured γ rays from the $^2H(\alpha,\gamma)^6Li$ reaction. Its signals were processed by a digital Caen N1827B module providing also list-mode data, and simultaneously by an Ortec 919E EtherNIM analog to digital converter and multichannel buffer as a backup solution and for comparison. The measured full-energy peak detection efficiency is plotted in fig. 2.
Inside the target, mainly the following nuclear reactions are expected to take place:

$$\begin{aligned} {}^2H(\alpha,\gamma)^6Li & \qquad Q = 1.474\,\text{MeV} \ (\text{R1}) \\ {}^2H(\alpha,\alpha)^2H \longrightarrow {}^2H(d,n)^3He & \qquad Q = 3.267\,\text{MeV} \ (\text{R2}) \\ \longrightarrow {}^2H(d,p)^3H & \qquad Q = 4.033\,\text{MeV} \ (\text{R3}) \end{aligned}$$

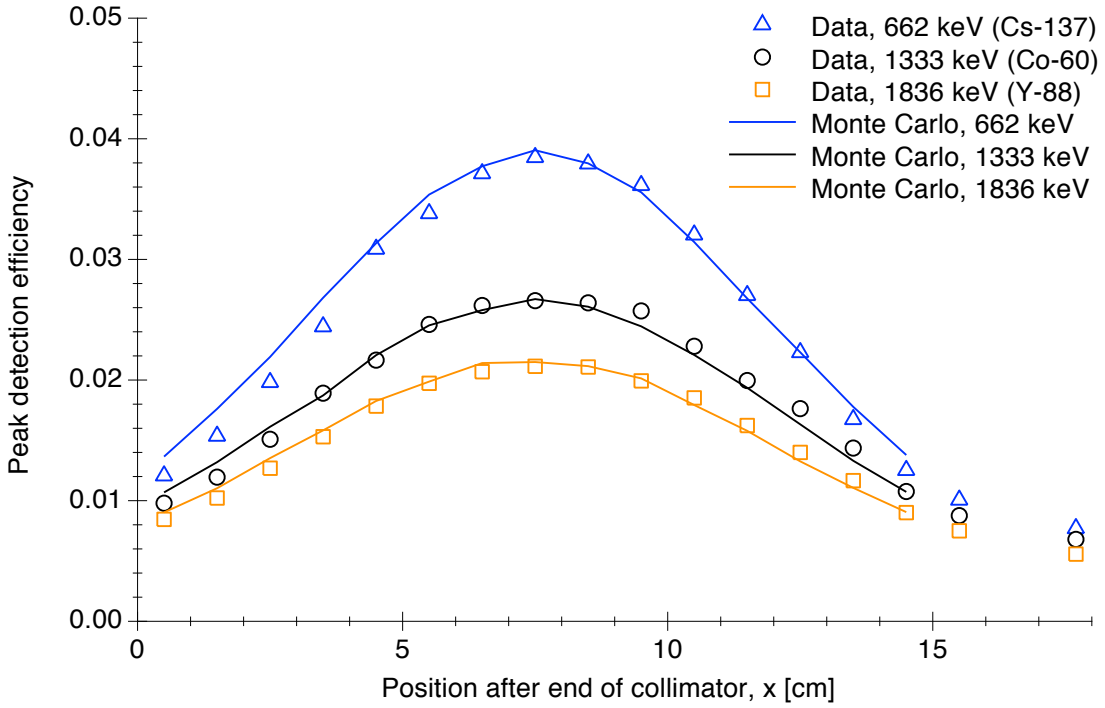

Figure 2: Full-energy peak detection efficiency measured with several calibrated γ-ray sources, as a function of the position *x* after the end of the final collimator. The efficiency from the GEANT4 Monte Carlo simulation is also shown for several positions.

Along with the reactions, also their *Q*-values are listed. Reaction R1 is the main reaction to be studied. Reactions R2 and R3 are parasitic reactions induced by elastically scattered deuterons with a ^{4}He beam incident on the gas target. As these deuterons have a maximum energy of only 356 keV (for E_α = 400 keV), other deuteron-induced reactions are negligible due to suppression by the Coulomb barrier. However, there is no Coulomb barrier for the energetic neutrons released by reaction R2, and the protons released by reaction R3 have an average energy of 3 MeV. Therefore, these protons and neutrons may give rise to further reactions on the structural material of the gas target system and on the detector material. The cross sections of these two conjugate reactions are similar, and they have nearly the same energy dependence at the energies relevant here [46]. As a consequence, the easily detectable protons from reaction R3 may be used to approximately infer also the yield of reaction R2. Knowing these boundary conditions, a steel tube (18 mm in diameter) surrounded the beam inside the target chamber to reduce the mean free path of protons and scattered deuterons. A silicon detector (1500 μm thick, 450 mm^2 active area) centered right above the HPGe detector measured the proton flux and thus indirectly the neutron flux, which was determined to be 10 neutrons per second.

For the experiment, the γ regions of interest are determined as follows. The ^{2}H(α,γ)^{6}Li reaction gives rise to a single γ ray at energy

$$E_\gamma = Q + E_{\mathrm{CM}} \pm \Delta E_{\mathrm{Doppler}} - \Delta E_{\mathrm{Recoil}} \tag{2.1}$$

The γ-ray energy shift due to the recoiling compound nucleus is negligible here, $\Delta E_{\mathrm{Recoil}} = 0.2$ keV. The Doppler correction, however, is significant, with the full Doppler shift amounting to $\Delta E_{\mathrm{Doppler}} \approx 16$ keV at $E_\alpha = 400$ keV. As the target is extended over and beyond the full diameter of the germanium detector leading to emissions before and behind the detector (fig. 1), the γ rays, including their flanks, fall into a region of interest (ROI) that ranges from 1552.5-1581.5 keV for E_α = 280 keV, and from 1589.5-1624.3 keV for E_α = 400 keV. The respective contributions of electric dipole and electric quadrupole capture to the cross section are known only from theory [15, 20]. Therefore, the angular distribution of the emitted γ rays is highly uncertain. Because of the strong Doppler effect, the unknown angular distribution translates into an unknown shape of the γ-peak. In order to be insensitive to the transition type (dipole or quadrupole), the entire region of interest is used.
In order to reduce the laboratory background, the γ-detector was surrounded by a lead shield with at least 20 cm of thickness in all directions. In this way, the γ-rate in the $^2H(\alpha,\gamma)^6Li$ ROI was reduced by a factor of 1100 with respect to an unshielded setup. Remaining laboratory background lines come from ^{40}K and the nuclides of the ^{238}U and ^{232}Th decay chain.

3. Observations with the germanium γ-ray detector with beam

Due to the parasitic reactions R2 and R3, a certain amount of unwanted energetic neutrons, protons, tritons, and ^3He particles are produced. They, in turn, may be captured by some structural, shielding or detector material. Energetic neutrons cause two main categories of effects in the setup. The first consists of capture and scattering effects on structural and shielding materials. They give rise to a number of well-defined γ rays with Gaussian shape (fig. 3). The detector end-cap consists of electrolytic copper, and the beam stop also consists of copper. A number of lines from the two stable copper isotopes $^{63,65}Cu$ are indeed observed (red markers in fig. 3) [52]. The gas target chamber consists of AISI 304 steel, and related neutron-induced lines from scattering on $^{54,56}Fe$ [55], ^{58}Ni and ^{52}Cr are apparent (grey and turquoise markers in fig. 3). At 803 keV, a line from neutron scattering on ^{206}Pb from the massive lead shield surrounding the target chamber is observed.

The second main effect is caused by (n,n'γ) processes of energetic neutrons on the germanium detector material itself. In addition to the emission of a γ ray from the deexcitation of an excited nuclear state in the germanium target nucleus, the recoiling target nucleus also deposits energy in the detector material [26], leading to a characteristic triangular shape starting at the energy of the γ ray. The broad features due to this effect (fig. 3) can be attributed to a number of excited states in several stable germanium isotopes. The ^{71m}Ge metastable state at E_x = 198 keV is a special case. It is excited by the $^{70}Ge(n,\gamma)$ reaction [23, 29]. Due to its long half-life of 20 ms, ^{71m}Ge decays only after the recoiling nucleus has been stopped. The ^{71m}Ge level at 198 keV decays via the 175 keV state in ^{71}Ge and onward to the ground state. The sum of these two γ rays gives rise to a Gaussian peak at 198 keV γ-ray energy in the spectrum (fig. 3).
The in-beam spectra display very similar features for the two beam energies E_α = 280 and 400 keV. The reason for this is that the maximum neutron energy varies not very much with beam energy, from 3.3 MeV at E_α = 400 keV to 3.1 MeV at E_α = 280 keV. The mutual similarity of the two

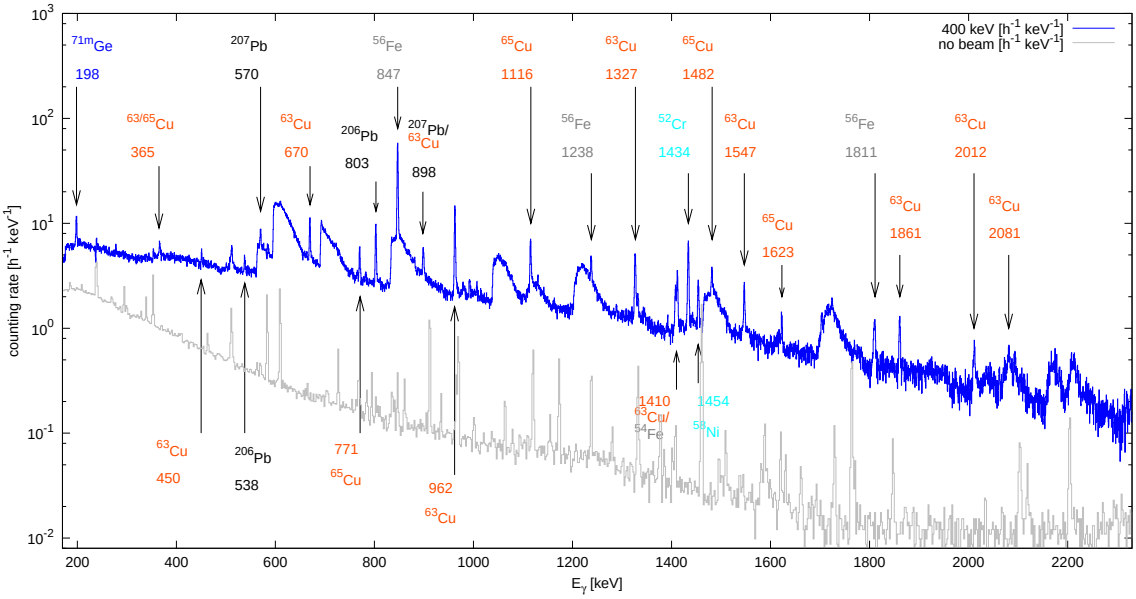

Figure 3: Spectra taken with the germanium detector. Blue full line: in-beam spectrum at E_α = 400 keV, p_{Target} = 0.3 mbar, laboratory background subtracted. The quantity plotted is the counting rate [h^{-1} keV^{-1}]. In order to obtain the yield [C^{-1} keV^{-1}], the values plotted have to be divided by 1.12 C/h. Grey thin line: Laboratory background. The most important in-beam lines due to (n,n'γ) and (n,γ) processes on structural and shielding materials are marked with arrows, and the relevant target nuclide is given, as well as the γ-ray energy in keV. The asymmetric lines are due to (n,n'γ) processes in the germanium detector itself.

neutron-induced spectra is actually closer than the similarity between the experimental spectrum at E_α = 280 keV and the simulated spectrum at the same energy.

4. Monte-Carlo simulations of the beam induced γ-background

A Monte Carlo simulation based on GEANT4 has been prepared. The full setup geometry is included, and the response of the HPGe detector is calculated in several steps: First, a deuteron energy distribution is gained from Rutherford scattering of incident α particles. Second, the deuteron-deuteron-reaction R2 yields a neutron energy spectrum. Third, the neutrons interact with setup materials, and the γ-ray emission is simulated. The agreement with the measured in-beam spectrum is very good with a few exceptions. Two remarkable examples are mentioned:

1. The Gaussian sum peak denoting the ^{71m}Ge metastable state at E_x = 198 keV [23, 29] is observed in the experiment, but not in the simulation. This is due to the well known GEANT4 problem that while the decay of metastable states is correctly handled by the `G4RDM` module, they are not correctly produced by the inelastic capture module. The 198 keV state lives so long that the recoiling ^{71m}Ge is completely stopped long before it decays, so the typical neutron triangle structure does not apply. A peak at the same energy may also be caused by the ^{19}F(n,n'γ) reaction, but this would require an unplausibly high amount of fluorine near the detector.

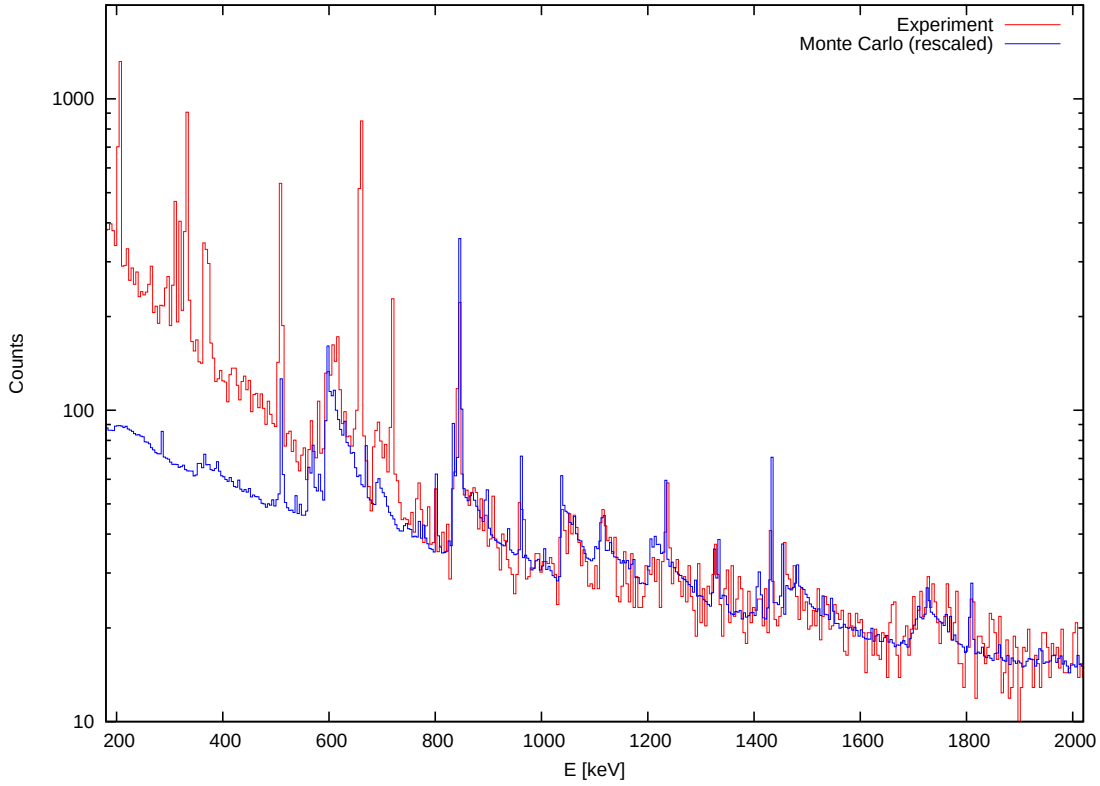

Figure 4: Spectrum of the AmBe neutron source from the experiment and from the Monte Carlo simulation.

2. The neutron triangle at 691 keV is much smaller in the simulation than in the data. The 0^+ excited state at E_x = 691 keV in ^{72}Ge decays exclusively by internal conversion to the 0^+ ground state, meaning its energy is detected in the present large germanium detector with an efficiency close to 1. The Monte Carlo simulation erroneously treats this level as decaying by γ-ray emission, meaning the γ ray is detected only with the intrinsic efficiency of the detector, which is considerably smaller than 1.

In order to check the response of the setup with a second type of neutron source, a weak americium-beryllium (Am-Be) neutron source, emitting MeV neutrons by the ^{9}Be(α,n)^{12}C reaction, was introduced to the setup. The ^{241}Am activity was 185 kBq, leading to an estimated neutron source strength of 13 n/s. It was placed in the center of the target chamber. Due to restrictions on the use of neutron sources in the LNGS underground facility, the running time was only 10 hours, limiting the statistical precision of the data. Therefore, the data had to be rebinned in order to make the spectra comparable, and any comparison by necessity concentrates on the general features of the spectrum (fig. 4). The triangular feature at 691 keV is not well reproduced in the simulation, for the reasons already discussed. At lower energies, $E_\gamma < 500$ keV, the simulation significantly underpredicts the data. This is due to the Compton continuum from the γ rays at 662 and 722 keV that are emitted by the ^{241}Am in the Am-Be source. These weak γ-ray branches of ^{241}Am are not included in the Monte Carlo simulation. In addition to energetic neutrons from the ^{9}Be(α,n)^{12}C reaction, an Am-Be source also emits Doppler-broadened 4.4 MeV γ rays from the decay of the first excited state of ^{12}C. These γ rays were not included in the Monte Carlo simulation, but they have

only a very limited influence near the ROIs for the $^2H(\alpha,\gamma)^6Li$ reaction. Overall, the spectrum from the Am-Be source is well reproduced by the simulation, including the neutron triangles except for the 691 keV one discussed below.

5. Outlook

The LUNA measurement campaign for the $^2H(\alpha,\gamma)^6Li$ experiment is completed, and the data analysis is underway. Another experiment to study the response of HPGe detectors in a neutron field induced by the $^2H(d,n)^3He$ reaction with high statistics has been carried out at the ELBE facility at Helmholtz-Zentrum Dresden-Rossendorf recently.
Even though the γ-background is one order of magnitude larger than the expected signal, the present data indicate that a positive measurement may be possible. A possible approach to parameterize the background in order to subtract it is currently under development.
Financial support by INFN, FAI, DFG (BE 4100-2/1), and NAVI is gratefully acknowledged.

References

[1] B. D. Fields, Annu. Rev. Nucl. Part. Sci. **61**, 47 (2011).

[2] A. J. Korn *et al.*, Nature **442**, 657 (2006), arXiv:astro-ph/0608201.

[3] M. Asplund, D. L. Lambert, P. E. Nissen, F. Primas, and V. V. Smith, Astrophys. J. **644**, 229 (2006).

[4] A. E. García Pérez *et al.*, Astron. Astrophys. **504**, 213 (2009), 0909.5163.

[5] M. Steffen, R. Cayrel, P. Bonifacio, H. Ludwig, and E. Caffau, Convection and ^{6}Li in the atmospheres of metal-poor halo stars, , IAU Symposium Vol. 268, pp. 215–220, 2010, 1001.3274.

[6] V. V. Smith, D. L. Lambert, and P. E. Nissen, Astrophys. J. **408**, 262 (1993).

[7] M. Steffen *et al.*, ArXiv e-prints **1206.2239** (2012).

[8] P. D. Serpico *et al.*, J. Cosmol. Astropart. Phys. **2004**, 010 (2004).

[9] N. Prantzos, Astron. Astrophys. **448**, 665 (2006).

[10] F. Iocco and M. Pato, Phys. Rev. Lett. **109**, 021102 (2012).

[11] M. Kusakabe, T. Kajino, and G. J. Mathews, Phys. Rev. D **74**, 023526 (2006).

[12] M. Pospelov, Phys. Rev. Lett. **98**, 231301 (2007).

[13] K. Jedamzik and M. Pospelov, New Journal of Physics **11**, 105028 (2009), 0906.2087.

[14] M. Pospelov and J. Pradler, Annu. Rev. Nucl. Part. Sci. **60**, 539 (2010), 1011.1054.

[15] L. Marcucci, K. Nollett, R. Schiavilla, and R. Wiringa, Nucl. Phys. A **777**, 111 (2006).

[16] P. Mohr *et al.*, Phys. Rev. C **50**, 1543 (1994).

[17] R. G. H. Robertson *et al.*, Phys. Rev. Lett. **47**, 1867 (1981).

[18] F. E. Cecil, J. Yan, and C. S. Galovich, Phys. Rev. C **53**, 1967 (1996).

[19] J. Kiener *et al.*, Phys. Rev. C **44**, 2195 (1991).

[20] F. Hammache *et al.*, Phys. Rev. C **82**, 065803 (2010), 1011.6179.

[21] G. Baur and H. Rebel, Annu. Rev. Nucl. Part. Sci. **46**, 321 (1996).

[22] C. Chasman, K. W. Jones, and R. A. Ristinen, Nucl. Inst. Meth. **37**, 1 (1965).

[23] R. Bunting and J. J. Kraushaar, Nucl. Inst. Meth. **118**, 565 (1974).

[24] G. Fehrenbacher, R. Meckbach, and H. G. Paretzke, Nucl. Inst. Meth. A **372**, 239 (1996).

[25] G. Fehrenbacher, R. Meckbach, and H. G. Paretzke, Nucl. Inst. Meth. A **397**, 391 (1997).

[26] J. Ljungvall and J. Nyberg, Nucl. Inst. Meth. A **546**, 553 (2005).

[27] A. Ataç *et al.*, Nucl. Inst. Meth. A **607**, 554 (2009), 0906.1232.

[28] I. Abt *et al.*, Eur. Phys. J. A **36**, 139 (2008), 0711.2255.

[29] G. Heusser, Nucl. Inst. Meth. B **83**, 223 (1993).

[30] G. Heusser, Annu. Rev. Nucl. Part. Sci. **45**, 543 (1995).

[31] R. Wordel *et al.*, Nucl. Inst. Meth. A **369**, 557 (1996).

[32] S. P. Ahlen *et al.*, Phys. Lett. B **249**, 149 (1990).

[33] P. Belli *et al.*, Nuovo Cimento A **101**, 959 (1989).

[34] F. Arneodo *et al.*, Nuovo Cimento A **112**, 819 (1999).

[35] H. Costantini *et al.*, Rep. Prog. Phys. **72**, 086301 (2009).

[36] C. Broggini, D. Bemmerer, A. Guglielmetti, and R. Menegazzo, Annu. Rev. Nucl. Part. Sci. **60**, 53 (2010).

[37] D. Bemmerer *et al.*, Eur. Phys. J. A **24**, 313 (2005).

[38] A. Caciolli *et al.*, Eur. Phys. J. A **39**, 179 (2009).

[39] T. Szücs *et al.*, Eur. Phys. J. A **44**, 513 (2010).

[40] A. Formicola *et al.*, Nucl. Inst. Meth. A **507**, 609 (2003).

[41] C. Casella *et al.*, Nucl. Inst. Meth. A **489**, 160 (2002).

[42] G. Gyürky *et al.*, Phys. Rev. C **75**, 035805 (2007).

[43] J. Görres, K. Kettner, H. Kräwinkel, and C. Rolfs, Nucl. Inst. Meth. **177**, 295 (1980).

[44] M. Marta *et al.*, Nucl. Inst. Meth. A **569**, 727 (2006).

[45] J. Osborne *et al.*, Nucl. Phys. A **419**, 115 (1984).

[46] D. S. Leonard, H. J. Karwowski, C. R. Brune, B. M. Fisher, and E. J. Ludwig, Phys. Rev. C **73**, 045801 (2006), arXiv:nucl-ex/0601035.

[47] D. Bemmerer *et al.*, Phys. Rev. Lett. **97**, 122502 (2006).

[48] F. Confortola *et al.*, Phys. Rev. C **75**, 065803 (2007).

[49] H. Costantini *et al.*, Nucl. Phys. A **814**, 144 (2008).

[50] C. Arpesella *et al.*, Nucl. Inst. Meth. A **360**, 607 (1995).

[51] S. Agostinelli *et al.*, Nucl. Inst. Meth. A **506**, 250 (2003).

[52] J. K. Dickens, Nucl. Phys. A **401**, 189 (1983).

[53] J. K. Dickens, Phys. Rev. C **28**, 916 (1983).

[54] M. Kadi *et al.*, Phys. Rev. C **61**, 034307 (2000).

[55] J. Lachkar, J. Sigaud, Y. Patin, and G. Haouat, Nucl. Phys. A **222**, 333 (1974).

[56] J. K. Dickens, Nucl. Sci. Eng. **50**, 311 (1973).

[57] P. Karatzas *et al.*, Nucl. Sci. Eng. **67**, 34 (1978).

[58] Evaluated Nuclear Structure Data File (ENSDF), International Atomic Energy Agency, http://www-nds.iaea.org/queryensdf.